Dispersion and Major Property Enhancements in Polymer/Multiwall Carbon Nanotube Nanocomposites via Solid-State Shear Pulverization Followed by Melt Mixing

Jun'ichi Masuda[†] **and John M. Torkelson***[,†,‡]

Department of Chemical and Biological Engineering and Department of Materials Science and Engineering, Northwestern University, Evanston, Illinois 60208

Received June 11, 2008
Revised Manuscript Received July 7, 2008

Introduction. Intense research has been focused on polymer nanocomposites because of their potential to dramatically enhance properties relative to neat polymer and to yield multifunctional materials.[1–36] Since their discovery in the early 1990s,[37] carbon nanotubes (CNTs) have been extensively studied as nanofillers[1–26] because of their low density, high aspect ratio, and excellent mechanical, electrical, and thermal properties. However, major challenges remain in polymer/CNT nanocomposites, especially related to CNT dispersion via industrially scalable, environmentally friendly methods and understanding the relationship between dispersion and optimal properties. Several strategies have been studied to achieve well-dispersed polymer/CNT nanocomposites, including melt mixing,[7–15] polymer/CNT blending in solvent (often with surface functionalization and/or sonication pretreatment),[16–21] and in situ polymerization.[22–24] Use of melt mixing alone often leads to limited CNT dispersion in polymer. Blending polymer and CNTs in solvent or in situ polymerization can lead to better dispersion, but the former method is not environmentally friendly and both methods have limited applicability and scalability.

Here we employ a continuous, solventless, scalable process called solid-state shear pulverization (SSSP)[26,27,38–43] in conjunction with melt mixing (MM) to produce well-dispersed polymer/multiwall CNT (MWCNT) nanocomposites. With SSSP, continuously generated deformation energy can be partially stored in the solid-state material and then released by creating new surfaces, resulting in dispersion. We have previously shown that SSSP with accompanying mechanochemical effects can result in nanoscale mixing free from thermodynamic limitations,[43] immiscible blend compatibilization by in situ block copolymer formation,[39–41] and debundling/exfoliation of nanoparticles in nanocomposites.[26,27] Limited, related effects have been observed with batch, solid-state processing.[25,32,44–46] In particular, using a solventless, two-step SSSP-plus-MM process, we show that heavily entangled, unmodified MWCNTs can be well dispersed in polypropylene (PP). We achieve 50−57% increases in Young's modulus, the largest improvement in Young's modulus ever reported for unoriented, isotactic PP/MWCNT nanocomposites.

Experimental Section. Polypropylene (Total Petrochemicals; MI = 2.0 g/10 min at 503 K and density of 0.905 g/cm^3, reported by supplier) and two types of MWCNT (Cheap Tubes; CNT-1 and CNT-2 with 30−50 nm and <8 nm outer diameters and 10−20 μm and 10−30 μm lengths, respectively, and 95+% purity, reported by supplier) were used as received. Dry-blended PP/CNT (1.0 wt %) mixtures were fed to a Berstorff ZE-25P pulverizer with conditions (feed rate, screw speed, screw design, ~273−290 K barrel temperature) selected to optimize CNT dispersion for a range of conditions studied. References 40 and 43 provide details on SSSP processing and equipment. Melt mixing of the SSSP product was done at 473 K in a cup-and-rotor mixer (Atlas Electronic Devices MiniMAX molder) for 15 min at maximum rotor speed with three steel balls in the cup.[47,48] Hybrids made by SSSP or MM only used similar conditions and CNT content.

Field-emission scanning electron microscopy (FE-SEM) and tensile samples were prepared by compression molding at 493 K (see Supporting Information). Tensile properties (Sintech 20/G) were measured following ASTM D1708. Morphologies of CNTs and cryo-fractured cross-sections were obtained via FE-SEM (Hitachi S4800; 3 kV) after sputter coating (Cressington 208HR) with gold/palladium. Isolated CNTs character-

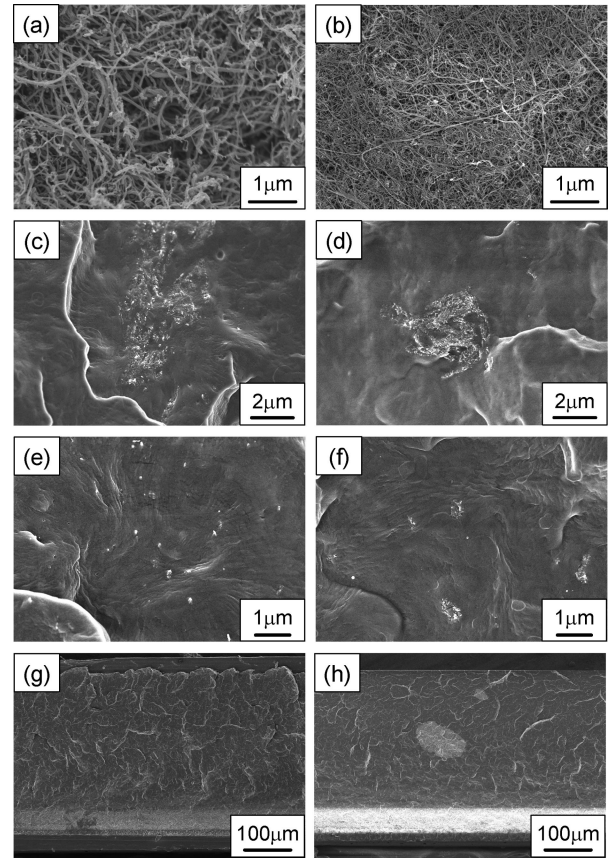

Figure 1. Field-emission scanning electron micrographs of carbon nanotubes and nanocomposites: (a) as-received CNT-1 and (b) as-received CNT-2, showing their highly entangled natures; (c) 99/1 wt % PP/CNT-1 and (d) 99/1 wt % PP/CNT-2 made by SSSP only − small white spots indicate ends of carbon nanotubes; (e) 99/1 wt % PP/CNT-1 and (f) 99/1 wt % PP/CNT-2 made by SSSP followed by melt mixing−small white spots indicate ends of carbon nanotubes; low magnification views of 99/1 wt % PP/CNT-1 indicating (g) the absence of large agglomerates in samples made by SSSP followed by melt mixing and (h) the presence of 10−100 μm agglomerates (whitish ovals in the micrograph) in samples made by melt mixing only. (Note: Micrographs c−h were taken on cryo-fractured surfaces. See Table 1 for exact CNT content in each nanocomposite or hybrid.)

* To whom correspondence should be addressed. E-mail: j-torkelson@northwestern.edu.
[†] Department of Chemical and Biological Engineering, Northwestern University.
[‡] Department of Materials Science and Engineering, Northwestern University.

10.1021/ma801321j CCC: $40.75
Published on Web 07/22/2008

Table 1. Mechanical Properties and Degradation Temperatures (Evaluated at 5% Mass Loss by TGA) for Neat PP and PP/CNT-1[49] and PP/CNT-2[49] Systems As a Function of Process Method[a]

system	processing	Young's modulus (GPa)	yield strength (MPa)	strain at break (%)	stress at break (MPa)	T_{deg} (°C)
none	PP as obtained	1.03 ± 0.05	31.3 ± 0.8	790 ± 30	44.1 ± 2.2	407
PP/ CNT-1	MM only (1.0 wt %)[b]	1.26 ± 0.02	33.3 ± 0.0	283 ± 258	30.4 ± 5.0	424
	SSSP only (0.93 wt %)[b]	1.40 ± 0.03	36.2 ± 0.2	841 ± 38	50.4 ± 2.0	422
	SSSP/MM (0.93 wt %)[b]	1.54 ± 0.02	39.3 ± 0.7	663 ± 83	42.6 ± 3.7	434
PP/ CNT-2	MM only (1.1 wt %)[b]	1.34 ± 0.01	34.7 ± 0.3	38 ± 57	28.3 ± 8.9	428
	SSSP only (0.92 wt %)[b]	1.44 ± 0.03	36.8 ± 0.6	793 ± 52	47.8 ± 2.5	434
	SSSP/MM (0.92 wt %)[b]	1.62 ± 0.03	40.8 ± 0.9	673 ± 93	45.4 ± 5.2	446

[a] Note: Exact CNT content for each nanocomposite or hybrid was determined by TGA. [b] Exact values of CNT content in resulting nanocomposites and hybrids as measured by thermogravimetric analysis.

ized by FE-SEM were prepared by making a CNT suspension in 50/50 w/w deionized water/2-propanol via low-level bath-type sonication (Branson 1200) for 1.5 h with poly(sodium 4-styrenesulfonate) (Aldrich) as dispersant and casting on plasma-treated Si wafers. Crystallization was measured at 411 K by differential scanning calorimetry (DSC; Mettler Toledo 822e) after annealing at 513 K for 5 min and quenching (50 K/min) to 411 K. The degradation temperature, T_{deg}, and CNT content[49] were measured by thermogravimetric analysis (TGA; Mettler Toledo 851e) in nitrogen atmosphere.

Results and Discussion. Figure 1 shows morphologies of as-received CNT-1 and CNT-2 and the 99/1 wt % PP/CNT-1[49] and 99/1 wt % PP/CNT-2[49] hybrids after SSSP, after SSSP followed by MM, and after MM only. As-received CNTs are in ~10 μm minimum-size agglomerates (see Supporting Information). Parts a and b of Figure 1 illustrate the heavily entangled nature of CNTs within these agglomerates, especially CNT-2. In nanocomposites made by SSSP, the CNT agglomerates are sharply reduced in size, forming loose structures interpenetrated by PP (Figure 1, parts c and d). Subsequent MM yields finer dispersion, with CNT-1 almost fully debundled into individual tubes and CNT-2 as individual tubes or in sub-500 nm diameter, loose agglomerates (Figure 1, parts e and f). These results indicate that two-step SSSP-plus-MM processing yields dispersion that is a function of CNT dimensions and entanglements in the as-received state. Thus, to achieve excellent dispersion, the two-step process must be tailored to CNT characteristics. In contrast, MM alone leads to little or no CNT dispersion. Parts g and h of Figure 1 compare the absence of agglomerates in PP/CNT-1 made by two-step processing with the presence of 10−100 μm agglomerates in PP/CNT-1 made via MM.

These conclusions are reinforced by PP crystallization kinetics. Figure 2a shows that isothermal crystallization of PP/CNT-1 systems at 411 K occurs much more rapidly than in neat PP because CNTs are nucleating agents for PP.[9,11,19–21,25] Due to poor dispersion, the melt-mixed hybrid exhibits the slowest crystallization of the PP/CNT-1 systems. The nanocomposite made by SSSP exhibits the broadest distribution of crystallization times, with the first 10% of relative crystallization occurring before 300 s and the last 5% occurring after 2200 s. This distribution likely originates from the inhomogeneous structure formed by SSSP, with loose CNT agglomerates interpenetrated by PP leading to rapid, local crystallization and isolated regions without CNTs to slow crystallization. In contrast, the nanocomposite made by two-step processing exhibits a symmetric, sharp crystallization curve, reflecting its homogeneous dispersion. The fact that this nanocomposite exhibits less than 2.5% relative crystallization at a 300 s crystallization time is consistent with the absence of loose CNT agglomerates. These results also indicate that characterization of isothermal crystallization half-time ($\tau_{1/2}$) without consideration of the crystallization-time

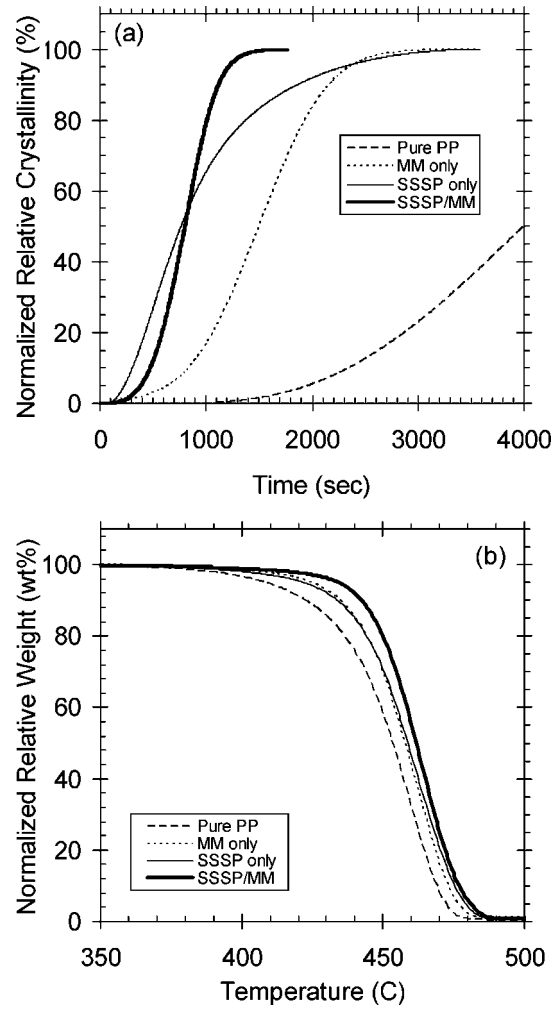

Figure 2. (a) Isothermal crystallization curves at 411 K and (b) thermogravimetric analysis data for neat PP and 99/1 wt % PP/CNT-1 nanocomposites as a function of process method. (Note: See Table 1 for exact CNT content in each nanocomposite or hybrid. Crystallinity levels achieved in neat PP and nanocomposites are the same within experimental error.)

distribution may lead to incorrect conclusions.[50] With the nanocomposite made by SSSP, $\tau_{1/2}$ = 760 s; with the nanocomposite made by two-step processing, $\tau_{1/2}$ = 820 s. Taken alone, these data may suggest that SSSP yields superior dispersion. However, the isothermal crystallization curves are consistent with superior dispersion by two-step processing.[50]

Figure 2b shows that polymer thermal stability improves with CNT dispersion. In neat PP, T_{deg} = 407 K. With PP/CNT-1, T_{deg} = 422 K when made by SSSP and 434 K when made by two-step processing. As shown in Table 1, higher T_{deg} values are obtained in PP/CNT-2, with the nanocomposite made by

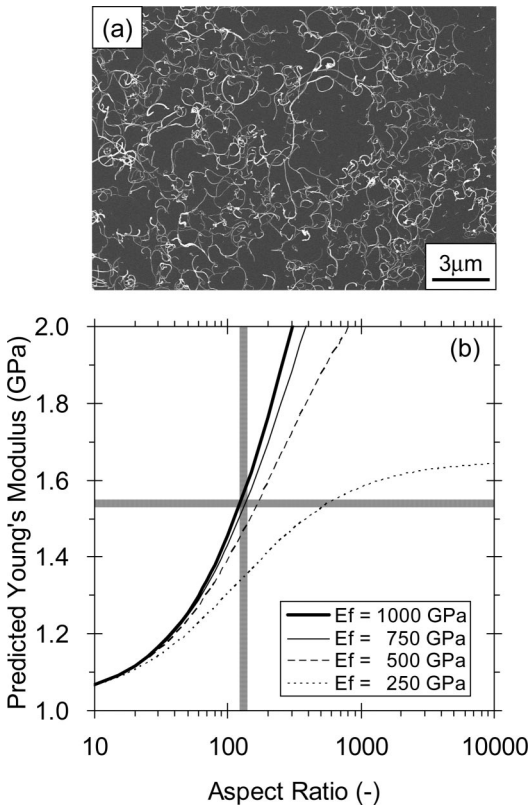

Figure 3. (a) Scanning electron micrograph showing polydispersity and waviness of individual CNT-1 nanotubes before processing with polymer. (b) Halpin−Tsai model predictions[51–54] of Young's modulus for PP nanocomposite (1 wt % nanotube) as a function of CNT aspect ratio. Vertical and horizontal gray lines indicate the experimentally estimated, representative aspect ratio of CNT-1 before processing and the experimentally measured Young's modulus for the 99/1 wt % PP/CNT-1 nanocomposite.

the two-step process yielding a 39 K increase in T_{deg} relative to neat PP. Thus, at equal CNT content, thermal stability is a function of CNT dispersion and diameter.

Table 1 compares the tensile properties of the nanocomposites with neat PP. The best property improvements are in nanocomposites made via two-step processing, with Young's modulus increasing by 50% and 57% and yield strength by 27% and 30% in PP/CNT-1 and PP/CNT-2, respectively. These increases in Young's modulus relative to neat PP are the largest reported in unoriented, isotactic PP/MWCNT nanocomposite films.[10,11,25] In contrast, hybrids made by MM exhibit much smaller improvements in Young's modulus and yield strength and major deteriorations in strain at break. (Among the samples listed in Table 1, differences in mechanical properties cannot be attributed to the levels of PP crystallinity, which are identical (46−49% via DSC) within experimental error.)

In order to compare the Young's modulus in PP/CNT-1 made by the two-step process to theoretical predictions for a nanocomposite with well-dispersed CNTs, we employed the Halpin-Tsai model for short-fiber-reinforced composites.[2,51] Micrographs such as Figure 3a indicate that, before processing, the CNT-1 lengths are 2−9 μm (smaller than the supplier-reported 10−20 μm),[52] resulting in a representative aspect ratio of ∼140.[53] This aspect ratio is represented by the vertical line in Figure 3b. The intersection of this line in Figure 3b with the Halpin-Tsai model curves[51,54] assuming a CNT density of 1.3 g/cm^3 (indicated as a minimum CNT density in ref 2) and CNT moduli of 750 and 1000 GPa yields an estimated theoretical upper bound of the modulus of PP/CNT-1 with homogeneously dispersed CNTs. The intersection indicates that the upper bound is ∼1.55 GPa, in excellent agreement with experiment (1.54 GPa). (Assumption of a CNT density exceeding 1.3 g/cm^3 yields a smaller predicted modulus from the Halpin−Tsai model, meaning that our experimentally measured modulus is equal to or greater than the value expected from the Halpin−Tsai model.)

Such quantitative agreement may reinforce conclusions that PP/CNT-1 is well dispersed and that CNTs do not undergo significant scission or shortening during SSSP. This agreement may also be considered surprising, because wavy CNTs should reduce the nanocomposite modulus in comparison to theory,[55] which assumes straight, well-dispersed CNTs. A possible explanation is related to the polymer−CNT interface. Ramanathan et al.[16] used the presence of rigid interfaces in well-dispersed poly(methyl methacrylate)/single-wall CNT nanocomposites to explain why the modulus exceeded the theoretically predicted upper bound. Solid-state shear pulverization of PP/CNT nanocomposites may lead to grafts of PP to the CNT, originating from macroradical formation.[41] Literature indicates that after Soxhlet extraction of PP/MWCNT and natural rubber/carbon black hybrids made by batch, solid-state processing,[25,56] the fillers were coated with polymer, potentially consistent with grafting polymer to filler. Any PP grafted to MWCNTs via SSSP would facilitate stress transfer at nanocomposite interfaces, enhancing Young's modulus. Investigation of these issues and studies as a function of CNT content, process conditions, and use temperature are underway in PP and other polymer nanocomposites, including polyethylene, poly(ethylene terephthalate), and high-performance engineering polymers. Comparisons with well-exfoliated graphite nanocomposites made by SSSP[27] are also planned.

Acknowledgment. We acknowledge support by Toray Industries and the NSF-MRSEC program (Grant DMR-0520513) and access to shared-user facilities managed by the Materials Research Center at Northwestern University and NUANCE.

Supporting Information Available: Additional text details on the experimental procedure and a figure showing the CNT microstructure before processing. This material is available free of charge via the Internet at http://pubs.acs.org.

References and Notes

(1) Ajayan, P. M.; Schadler, L. S.; Giannaris, C.; Rubio, A. *Adv. Mater.* **2000**, *12*, 750–753.
(2) Coleman, J. N.; Khan, U.; Blau, W. J.; Gun'ko, Y. K. *Carbon* **2006**, *44*, 1624–1652.
(3) Moniruzzaman, M.; Winey, K. I. *Macromolecules* **2006**, *39*, 5194–5205.
(4) Schaefer, D. W.; Justice, R. S. *Macromolecules* **2007**, *40*, 8501 8517.
(5) Winey, K. I.; Vaia, R. A. *MRS Bull.* **2007**, *32*, 314–319.
(6) Krishnamoorti, R. *MRS Bull.* **2007**, *32*, 341–347.
(7) Pegel, S.; Potschke, P.; Petzold, G.; Alig, I.; Dudkin, S. M.; Lellinger, D. *Polymer* **2008**, *49*, 974–984.
(8) Lin, B.; Sundararaj, U; Potschke, P. *Macromol. Mater. Eng.* **2006**, *291*, 227–238.
(9) Bhattacharyya, A. R.; Sreekumar, T. V.; Liu, T.; Kumar, S.; Ericson, L. M.; Hauge, R. H.; Smalley, R. E. *Polymer* **2003**, *44*, 2373–2377.
(10) Yang, J. L.; Zhang, Z.; Friedrich, K.; Schlarb, A. K. *Macromol. Rapid Commun.* **2007**, *28*, 955–961.
(11) Zhang, H.; Zhang, Z. *Eur. Polym. J.* **2007**, *43*, 3197–3207.
(12) Kharchenko, S. B.; Douglas, J. F.; Obrzut, J.; Grulke, E. A.; Migler, K. B. *Nat. Mater.* **2004**, *3*, 564–568.
(13) Li, Y. J.; Shimizu, H. *Polymer* **2007**, *48*, 2203–2207.
(14) Dondero, W. E.; Gorga, R. E. *J. Polym. Sci., Part B: Polym. Phys.* **2006**, *44*, 864–878.
(15) Gorga, R. E.; Cohen, R. E. *J. Polym. Sci., Part B: Polym. Phys.* **2004**, *42*, 2690–2702.
(16) Ramanathan, T.; Liu, H.; Brinson, L. C. *J. Polym. Sci., Part B: Polym. Phys.* **2005**, *43*, 2269–2279.

(17) Chang, T. E.; Jensen, L. R.; Kisliuk, A.; Pipes, R. B.; Pyrz, R.; Sokolov, A. P. *Polymer* **2005**, *46*, 439–444.
(18) Kashiwagi, T.; Fagan, J.; Douglas, J. F.; Yamamoto, K.; Heckert, A. N.; Leigh, S. D.; Obrzut, J.; Du, F. M.; Lin-Gibson, S.; Mu, M.; Winey, K. I.; Haggenmueller, R. *Polymer* **2007**, *48*, 4855–4866.
(19) Xu, D. H.; Wang, Z. G. *Polymer* **2008**, *49*, 330–338.
(20) Moore, E. M.; Ortiz; D, L.; Marla; V, T.; Shambaugh, R. L.; Grady, B. P. *J. Appl. Polym. Sci.* **2004**, *93*, 2926–2933.
(21) Avila-Orta, C. A.; Medellin-Rodriguez, F. J.; Davila-Rodriguez, M. V.; Aguirre-Figueroa, Y. A.; Yoon, K.; Hsiao, B. S. *J. Appl. Polym. Sci.* **2007**, *106*, 2640–2647.
(22) Putz, K. W.; Mitchell, C. A.; Krishnamoorti, R.; Green, P. F. *J. Polym. Sci., Part B: Polym. Phys.* **2004**, *42*, 2286–2293.
(23) Funck, A.; Kaminsky, W. *Compos. Sci. Technol.* **2007**, *67*, 906–915.
(24) Trujillo, M.; Arnal, M. L.; Mueller, A. J.; Bredeau, S.; Bonduel, D.; Dubois, P.; Hamley, I. W.; Castelletto, V. *Macromolecules* **2008**, *41*, 2087–2095.
(25) Xia, H. S.; Wang, Q.; Li, K. S.; Hu, G. H. *J. Appl. Polym. Sci.* **2004**, *93*, 378–386.
(26) Mu, M. F.; Walker, A. M.; Torkelson, J. M.; Winey, K. I. *Polymer* **2008**, *49*, 1332–1337.
(27) Wakabayashi, K.; Pierre, C.; Dikin, D. A.; Ruoff, R. S.; Ramanathan, T.; Brinson, L. C.; Torkelson, J. M. *Macromolecules* **2008**, *41*, 1905–1908.
(28) Ramanathan, T.; Stankovich, S.; Dikin, D. A.; Liu, H.; Shen, H.; Nguyen, S. T.; Brinson, L. C. *J. Polym. Sci., Part B: Polym. Phys.* **2007**, *45*, 2097–2112.
(29) Giannelis, E. P. *Adv. Mater.* **1996**, *8*, 29–35.
(30) Ray, S. S.; Okamoto, M. *Prog. Polym. Sci.* **2003**, *28*, 1539–1641.
(31) Potschke, P.; Fornes, T. D.; Paul, D. R. *Polymer* **2002**, *43*, 3247–3255.
(32) Saito, T.; Okamoto, M.; Hiroi, R.; Yamamoto, M.; Shiroi, T. *Macromol. Rapid Commun.* **2006**, *27*, 1472–1475.
(33) Rittigstein, P.; Torkelson, J. M. *J. Polym. Sci., Part B: Polym. Phys.* **2006**, *44*, 2935–2943.
(34) Rittigstein, P.; Priestley, R. D.; Broadbelt, L. J.; Torkelson, J. M. *Nat. Mater.* **2007**, *6*, 278–282.
(35) Podsiadlo, P.; Kaushik, A. K.; Arruda, E. M.; Waas, A. M.; Shim, B. S.; Xu, J. D.; Nandivada, H.; Pumplin, B. G.; Lahann, J.; Ramamoorthy, A.; Kotov, N. A. *Science* **2007**, *318*, 80–83.
(36) Capadona, J. R.; Van Den Berg, O.; Capadona, L. A.; Schroeter, M.; Rowan, S. J.; Tyler, D. J.; Weder, C. *Nat. Nanotech.* **2007**, *2*, 765–769.
(37) Iijima, S. *Nature* **1991**, *354*, 56–58.
(38) Khait, K.; Torkelson, J. M. *Polym.-Plast. Technol. Eng.* **1999**, *38*, 445–457.
(39) Furgiuele, N.; Lebovitz, A. H.; Khait, K.; Torkelson, J. M. *Macromolecules* **2000**, *33*, 225–228.
(40) Lebovitz, A. H.; Khait, K.; Torkelson, J. M. *Macromolecules* **2002**, *35*, 8672–8675.
(41) Lebovitz, A. H.; Khait, K.; Torkelson, J. M. *Macromolecules* **2002**, *35*, 9716–9722.
(42) Brinker, K. L.; Lebovitz; A, H.; Torkelson, J. M; Burghardt, W. R. *J. Polym. Sci., Part B: Polym. Phys.* **2005**, *43*, 3413–3420.
(43) Tao, Y.; Kim, J.; Torkelson, J. M. *Polymer* **2006**, *47*, 6773–6781.
(44) Huang, L. Q.; Pan, L. H.; Inoue, T. *J. Appl. Polym. Sci.* **2007**, *104*, 787–791.
(45) Smith, A.; Spontak, R. J.; Ade, H.; Smith, S. D.; Koch, C. C. *Adv. Mater.* **1999**, *11*, 1277–1281.
(46) Schexnaydre, R. J.; Mitchell, B. S. *Polym. Eng. Sci.* **2008**, *48*, 649–655.
(47) Maric, M.; Macosko, C. W. *Polym. Eng. Sci.* **2001**, *41*, 118–130.
(48) On the basis of the resulting dispersed-phase domain size, Maric and Macosko showed in ref 47 that melt mixing of immiscible polymer blends with a MiniMAX mixer containing three small steel balls can yield microstrucures with dispersion levels that are comparable to those attained with external, intensive batch mixers and twin-screw extruders. Similar dispersion relationships may be expected for polymer−CNT nanocomposites.
(49) For each hybrid or nanocomposite, we attempted to incorporate 1.0 wt % MWCNT. For simplicity, in the text we have indicated that our hybrids or materials are 99 wt % PP and 1 wt % CNT. We have obtained precise and accurate determinations of CNT content via thermogravimetric analysis, with CNT contents ranging from a low of 0.92 wt % for PP/CNT-2 made by SSSP or SSSP followed by melt mixing to a high of 1.1 wt % for PP/CNT-2 made by melt mixing only. Table 1 lists exact CNT contents.
(50) We note that the use and meaning of the term "superior dispersion" may depend on the application being considered. For example, regarding the enhancement of mechanical properties, such as considered in this manuscript, superior dispersion relates to the maximiziation of Young's modulus, which is expected if the nanotubes are dispersed homogeneously at the level of individual nanotubes. However, as shown in ref 26, when enhanced electrical conductivity is the goal, the development of a contigous, cellular CNT structure yielding electrical percolation can result in greater property enhancement than a relatively homogeneous CNT dispersion.
(51) Halpin, J. C.; Kardos, J. L. *Polym. Eng. Sci.* **1976**, *16*, 344–352.
(52) As the individual tubes associated with CNT-1 had wavy structures when cast on a Si wafer (Figure 3a), we were unable to use image analysis to determine tube lengths and instead estimated lengths by visual inspection of micrographs. The estimated 2−9 μm lengths of the as-received CNTs are lower than those reported by the supplier (10−20 μm). We believe that our values are correct because we obtained similar results using very different sonication times.
(53) To obtain representative values for the CNT-1 length and diameter, we used the value midway between the minimum and maximum, which are 2 and 9 μm for the length (from micrographs) and 30 and 50 μm for the diameter (reported by the supplier). The representative CNT-1 aspect ratio of 140 was obtained by dividing the intermediate value of the length by that of the diameter and rounding to two significant digits.
(54) For purposes of calculation, we used the following: 1.3 g/cm^3 CNT density, 0.91 g/cm^3 PP density, and 1.0 wt % CNT content.
(55) Fisher, F. T.; Bradshaw, R. D.; Brinson, L. C. *Compos. Sci. Technol.* **2003**, *63*, 1689–1703.
(56) Xu, H. Y.; Li, B. Y.; Wu, C. F. *Polym. J.* **2006**, *38*, 807–813.

MA801321J